

Electronic Supplementary Information

Self-interconnecting Pt Nanowire Network Electrode for Electrochemical Amperometric Biosensor

Shuqi Wang,^{a,b} Li-Ping Xu,^{a,b,*} Hai-Wei Liang,^d Shu-Hong Yu,^{d,*} Yongqiang Wen,^{a,b} Shutao Wang^{c,*} and Xueji Zhang^{a,b,*}

^aResearch Center for Bioengineering and Sensing Technology, University of Science & Technology Beijing, Beijing 100083, P.R. China.

^bSchool of Chemistry and Biological Engineering, University of Science and Technology Beijing, Beijing, 100083, P.R. China

^cLaboratory of Bioinspired Smart Interface Science, Technical Institute of Physics and Chemistry, Chinese Academy of Sciences, Beijing 100190, P.R. China

^dDivision of Nanomaterials and Chemistry, Hefei National Laboratory for Physical Sciences at Microscale, Department of Chemistry, the National Synchrotron Radiation Laboratory, University of Science and Technology of China, Hefei, Anhui 230026, P.R. China

*Address correspondence, Fax: 86-10-82375840; Tel: 86-10-82375840; E-mail: xuliping@ustb.edu.cn; stwang@mail.ipc.ac.cn; zhangxueji@ustb.edu.cn.

1)

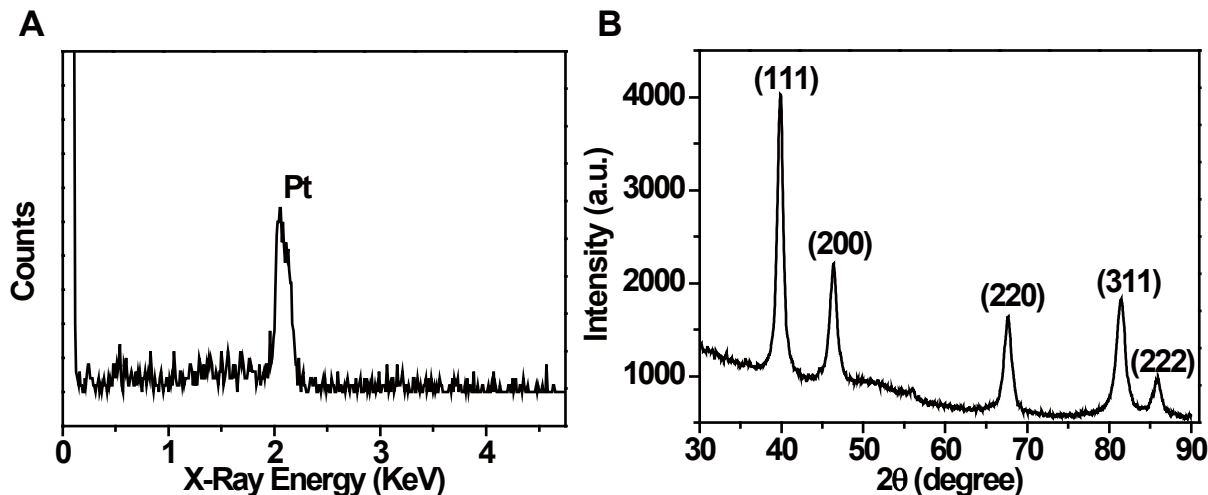


Fig. S1. (A) EDS spectrum of the Pt nanowires. (B) XRD pattern of PtNNE.

2)

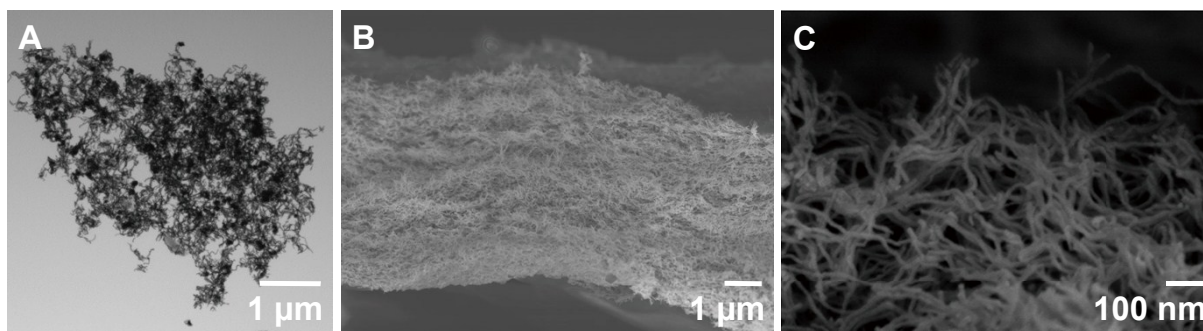


Fig. S2. (A) TEM image of PtNNE dispersed in ethanol by ultrasonic treatment. (B) Side-view SEM image and (C) the high-magnification SEM images of PtNNE.

3) The voltammetric behavior of PtNNE in response to 20 mM H_2O_2 in 0.1 M oxygen-free, air saturated, O_2 saturated PBS (pH 7.0) was shown in Fig. S3A. PtNNE exhibited an obvious reduction peak at -0.2 V in presence of H_2O_2 , revealing that the electrode has great electrocatalytic activity towards H_2O_2 . The bare GCE has no reduction peak upon addition of 20 mM H_2O_2 (not shown in paper), which confirmed that the electrocatalytic ability only attributed to PtNNE. A broad of reduction and oxidation peaks appeared at -0.5 to -1.0 V in Fig. S3A attributed to OH desorption/adsorption or reduction/oxidation of Pt-oxide.¹

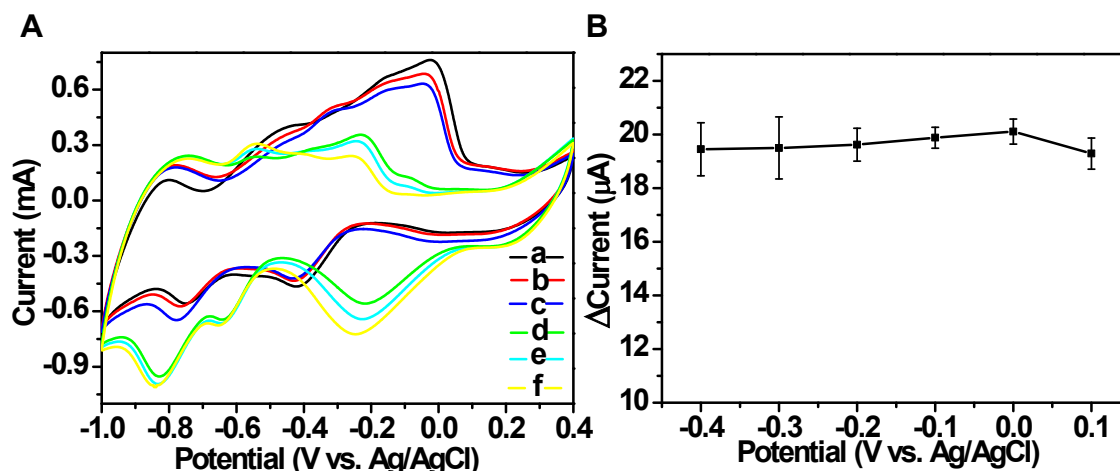


Fig. S3. (A) CV of PtNNE responses to 20 mM H₂O₂ in (a) in air saturated PBS; (b) in N₂ saturated PBS; (c) in O₂ saturated PBS; (d) 20 mM H₂O₂ in N₂ saturated PBS; (e) 20 mM H₂O₂ in air saturated PBS; (f) 20 mM H₂O₂ in O₂ saturated PBS. (B) Current responses of 200 μM H₂O₂ at different applied potentials in oxygen-free PBS.

For amperometric detection, it is important to select a proper detection potential to achieve high selectivity and sensitive current response. It is well known that the oxygen reduction commonly occurs at a negative potential. Comparing the CV responses of H₂O₂ in N₂ saturated, air saturated and O₂ saturated PBS (Fig. S3A), the reduction current of H₂O₂ increased in air and O₂ saturated PBS, indicating that the O₂ could be abundantly reduced below 0 V, which would increase the current response of H₂O₂. Fig. S3B compared the amperometric responses of PtNNE towards 200 μM H₂O₂ in N₂ saturated PBS at different applied potentials. As can be seen, a similar current change with a slight increase trend was observed at the potential range of -0.4 to 0 V, but an obvious decreasing current obtained when the potential shifted to positive value at 0.1 V. To get a better selectivity and sensitivity, the potential of 0 V was selected in this study, hence the oxygen reduction current can be limited and the responses of common interference species (include glucose, ascorbic acid, citric acid and uric acid) can be minimized (see Fig. S4).

The influences of common endogenous electroactive interferences at different potential were shown in Fig. S4. The responses of those interferences were minimized at the optimized potential of 0 V, for 1 mM ascorbic acid decreased by 8.1% compared with the current signal change of 1 mM H_2O_2 , 1 mM glucose decreased by 6.6%, 1 mM citric acid and 0.3 mM uric acid could hardly cause any current signal.

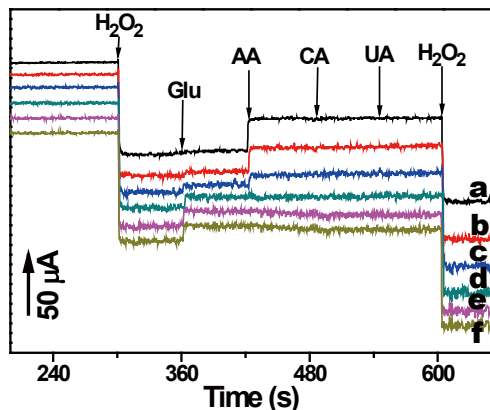


Fig. S4. The amperometry responses of PtNNE towards 1 mM H_2O_2 , 1 mM glucose (Glu), 1 mM ascorbic acid (AA), 1 mM citric acid (CA) and 0.3 mM uric acid (UA) at different applied potential range from (a) 0.2 V, (b) 0.1 V, (c) 0 V, (d) -0.1 V, (e) -0.2 V, (f) -0.3 V.

4) AFM images compared the surface morphology of PtNNE and PtNNE/GOx as shown in Fig. S5. Obviously, the surface of PtNNE/GOx turned smooth compared with the sharp bump surface of PtNNE. The roughness of PtNNE and PtNNE/GOx were 3.7 nm and 0.9 nm, respectively, which indicated the successful immobilization of GOx on PtNNE. The interactions between GOx and PtNNE were studied by infrared spectra. The FT-IR spectra of GOx and PtNNE/GOx were shown in Fig. S6. The spectrum of GOx showed two important infrared bands of amide I around 1650 cm^{-1} and amide II around 1542 , which are consistent with the feature of GOx in literature.² It could be observed that the spectrum of PtNNE/GOx was almost identical to that of GOx, which could indicate that the interactions between PtNNE and GOx were physically, and the bioactivity of GOx could be maintained.

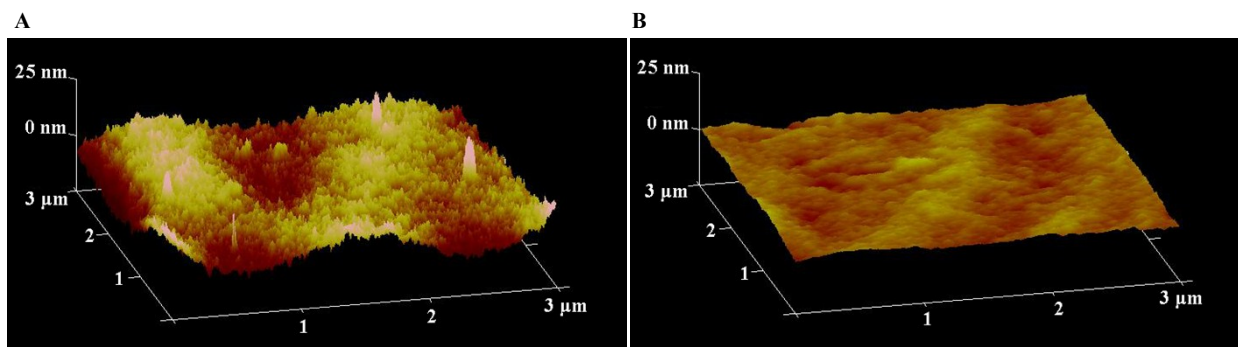


Fig. S5 AFM images of PtNNE (A) and PtNNE/GOx.

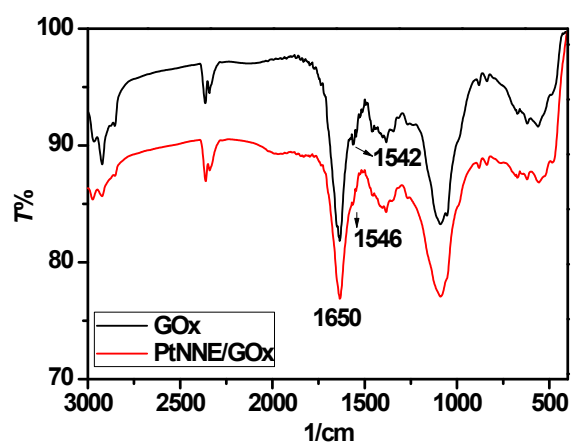


Fig. S6 FT-IR spectra of GOx and PtNNE/GOx.

5)

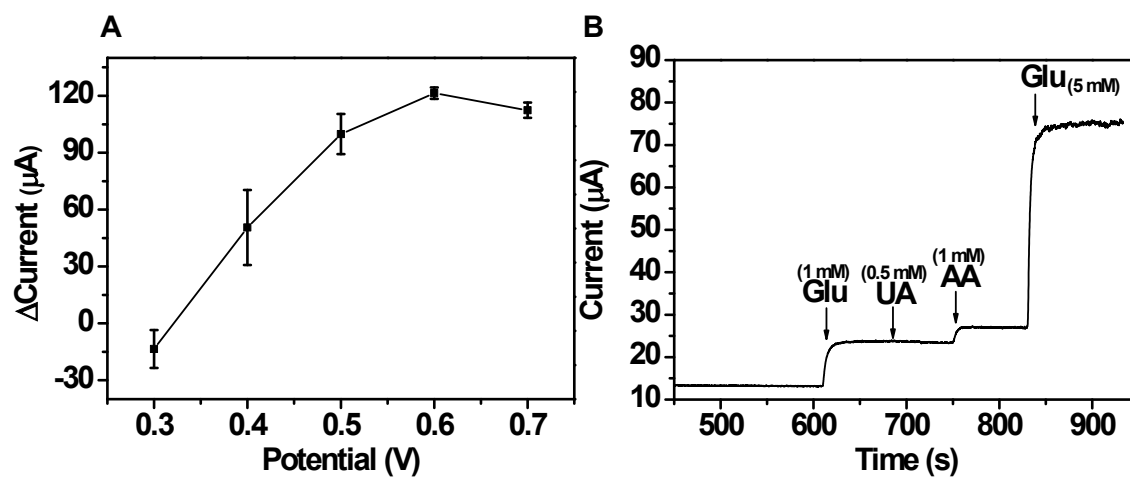


Fig. S7 (A) Current responses of PtNNE towards 1 mM H₂O₂ at different applied potentials in 0.1 M PBS. (B) Amperometry responses of PtNNE/GOx upon glucose, uric acid and ascorbic acid at 0.6 V in 0.1 M PBS.

6)

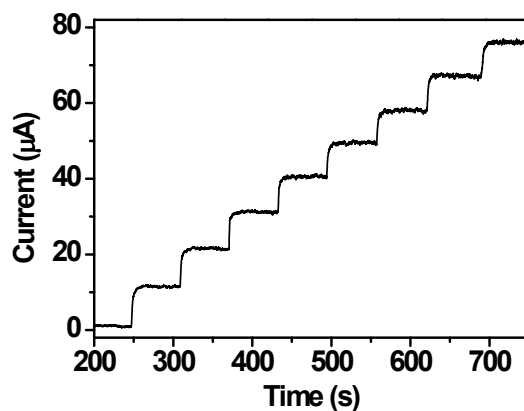


Fig. S8 Amperometry responses of PtNNE/GOx upon successive injections of 1 mM glucose into stirring 0.1 M PBS (pH 7.0) at applied potential of 0.6 V.

1. P. Karam and L. I. Halaoui, *Anal Chem*, 2008, **80**, 5441-5448.
2. C. Chey, Z. Ibupoto, K. Khun, O. Nur and M. Willander, *Sensors*, 2012, **12**, 15063-15077.